

## Simulated-tempering procedure for spin-glass simulations

Werner Kerler and Peter Rehberg

*Fachbereich Physik, Universität Marburg, D-35032 Marburg, Germany*

(Received 3 February 1994)

We develop an appropriate iteration procedure for the determination of the parameters for the method of simulated tempering and test it successfully on the two-dimensional Ising spin glass. The reduction of the slowing down is comparable to that of the multicanonical algorithm. Simulated tempering has, however, the advantages of allowing full vectorization of the programs and of providing the canonical ensemble directly.

PACS number(s): 02.70.-c, 05.50.+q, 11.15.Ha

### I. INTRODUCTION

A better theoretical understanding of spin glasses is still highly desirable. To make progress within this respect, more efficient simulation algorithms are needed. In particular, at low temperatures conventional simulations suffer from severe slowing down due to energy barriers. Recently, Berg and Celik [1] have been able to reduce the slowing down considerably by applying the multicanonical method [2]. Shortcomings of this method are that the computer programs cannot be vectorized and that additional calculations (with complicated error estimates) are needed to obtain the canonical ensemble.

An alternative is offered by the method of simulated tempering, which has been introduced by Marinari and Parisi [3] for the random-field Ising model. It works by associating a set of inverse temperatures to an additional dynamical variable of the Monte Carlo scheme. Because the system then is warmed up from time to time, one gets a chance to avoid the effective ergodicity breaking [4] observed in conventional approaches. By this method one gets the canonical ensemble directly at each of the temperatures and there is nothing that prevents vectorization of the programs.

In these simulations involving the joint probability distribution of the spins and of the additional variable, one has the freedom to choose the set of temperatures and the probability distribution of the additional variable. Fixing these quantities in an optimal way is crucial for the efficiency of the method. In the first application to the random-field Ising model on small lattices, this appeared to be not very demanding [3]. However, for spin glasses, in particular, for larger lattices and low temperatures, we find that the appropriate determination of these parameters is far from straightforward.

In the present paper, we discuss the related algorithmic possibilities and develop a systematic procedure which allows us to fix the respective parameters in an appropriate way. We test our method on the two-dimensional (2D) Ising spin glass and show that an efficient algorithm is obtained.

We use the Edwards-Anderson Hamiltonian with two replicas,

$$H(s, t) = - \sum_{\langle i, j \rangle} J_{ij} (s_i s_j + t_i t_j), \quad (1.1)$$

where the sum goes over nearest neighbors, and  $s_i = \pm 1$ ,  $t_i = \pm 1$ . Thus, we are able to measure the order parameter [4-6]

$$q = \sum_i s_i t_i. \quad (1.2)$$

We investigate samples for which  $J_{ij}$  is put equal to  $+1$  and  $-1$  with equal probability.

To each value of the additional dynamical variable  $n$  of simulated tempering, which takes the values  $1, 2, \dots, N$ , an inverse temperature  $\beta_n$  with  $\beta_1 < \beta_2 < \dots < \beta_N$  is associated. The partition function of the joint system then becomes

$$Z = \sum_{n, s, t} \exp[-\beta_n H(s, t) + g_n]. \quad (1.3)$$

The parameters  $g_n$  reflect the freedom in the choice of the probability distribution  $p(n)$  of the variable  $n$ .

Two steps are necessary in the calculations. In the first step, the parameters  $g_n$  and  $\beta_n$  are determined. Then in the second step, using these parameters, the simulations are performed and the physical observables are measured. The dynamical variables  $s_i$ ,  $t_i$ ,  $n$  are all updated by standard Metropolis [7] techniques. Slowing down is measured in terms of the ergodicity time  $\tau_E$  [1], which is defined as the mean time (in Monte Carlo sweeps) the system needs to travel from  $n = 1$  to  $N$  and back. Since decoupling of the spins is related to heating the system, this is an upper limit for the time one needs to get independent spin configurations.

In Sec. II, the iteration procedures for the determination of the parameters is described. Section III contains a discussion of the properties of this procedure. In Sec. IV, some numerical results are presented.

### II. ITERATION PROCEDURE

To choose  $p(n)$  constant as proposed in Ref. [3], i.e., to visit the states  $n$  with equal probability, appears reason-

able. In a similar approach [8], in which the additional dynamical variable is the number of components in the Potts model, it has turned out that such a choice is optimal. Constant  $p(n)$  in terms of the  $g_n$  means that

$$g_n = -\ln \tilde{Z}(\beta_n), \quad (2.1)$$

with the spin-glass partition function

$$\tilde{Z}(\beta) = \sum_{s,t} \exp(-\beta H(s,t)). \quad (2.2)$$

It should be noted that  $g_n$  depends on  $\beta_n$  only.

Our choice here is to come sufficiently close to (2.1). Because of the exponential dependence of  $p(n)$  on  $g_n$  the deviations from (2.1) must be small in order that all states  $n$  are appropriately reached. We use two methods to calculate the  $g_n$ . The first one is to replace  $g_n$  by  $g_n - \ln(Np(n))$  in subsequent iterations such that one ultimately arrives at constant  $p(n)$ . The second method is to apply reweighting [9] of the obtained distribution to get the ratio of the  $\tilde{Z}$  at neighboring  $n$  and thus by (2.1) the differences of the respective new  $g_n$ . The new  $g_n$  then are calculated from these differences.

To get hints on a reasonable choice of the  $\beta_n$ , one observes that the mean value of the logarithm of the acceptance probability  $\exp(-\Delta\beta H + \Delta g)$  to order  $(\Delta\beta)^3$  is

$$\left( \langle H^2 \rangle - \langle H \rangle^2 \right) (\Delta\beta)^2. \quad (2.3)$$

On this basis, one may require [3] choosing  $\beta_n$  in such a way that (2.3) gets as constant as possible. Then, due to  $\langle H^2 \rangle - \langle H \rangle^2 \sim L^2$  at fixed  $\beta$ , it follows that the number  $N$  of temperature values should scale like  $N \sim L$  on the  $L \times L$  lattice. Further, this indicates that at larger  $\beta$ , where  $\langle H^2 \rangle - \langle H \rangle^2$  is small, the distances between the  $\beta$  values should increase. Unfortunately, at low temperatures (large  $\beta$ ) the requirement to make (2.3) constant cannot be used to determine  $\Delta\beta$  because the measurements are likely to arrive at  $\langle H^2 \rangle - \langle H \rangle^2 = 0$ , which would result in a breakdown of an iterative determination of the  $\beta_n$ .

We propose to calculate the  $\beta_n$  by using a map which has an attractive fixed point. The map which we have constructed and applied has the property that if the fixed point is reached in a sequence of mappings, the effective stay time  $\tau_n^{\text{eff}}$  at a state  $n$  gets constant. This quantity is defined by

$$\tau_n^{\text{eff}} = \begin{cases} \frac{1}{2}\tau_n & , n = 1, N \\ \tau_n & , 2 \leq n \leq N-1 \end{cases} \quad (2.4)$$

where the stay time  $\tau_n$  is the mean time which elapses between entering state  $n$  and leaving it. To perform the map, we first compute the auxiliary quantities,

$$a_n = (\beta_{n+1} - \beta_n) / (\tau_{n+1}^{\text{eff}} + \tau_n^{\text{eff}}), \quad n = 1, \dots, N-1, \quad (2.5)$$

$$c = \sum_{n=1}^{N-1} a_n. \quad (2.6)$$

Then we get new values  $\beta'_n$  by

$$\beta'_1 = \beta_1, \quad (2.7)$$

$$\beta'_n = \beta'_{n-1} + a_{n-1} \frac{\beta_N - \beta_1}{c}, \quad n = 2, \dots, N. \quad (2.8)$$

Since  $\beta_1$  and  $\beta_N$  are mapped to themselves the region of  $\beta$  covered does not change. The fixed point gets attractive because a large stay time implies a smaller  $\beta$  difference and thus a smaller stay time in the next iteration step. The numerical results indicate that by the sequence of mappings also (2.3) gets very close to a constant value.

Our procedure, which determines the parameters in an iterative way, is started with equidistant  $\beta_n$  and with  $g_n$  estimated by the relation [10]  $g_n = -L^2 [a\beta_n + b \exp(-k\beta)] + c$ . Each iteration involves four steps: (1) An appropriate number (typically some multiple of the expected ergodicity time) of Monte Carlo sweeps are performed to obtain the necessary data, as, e.g.,  $p(n)$  and  $\tau_n$ . (2) New  $g_n$  are computed by one of the two methods indicated above. (3) The map described above is used to obtain new  $\beta_n$ . (4) New  $g_n$ , which are related to these  $\beta_n$  are determined by spline interpolation [11] (this step is dictated by the fact that  $g_n$  is a function of  $\beta_n$ ). Criteria for the termination of the iteration procedure are discussed in Sec. III.

### III. PROPERTIES OF THE PROCEDURE

To study the impact of the number  $N$  of  $\beta$  values, we have measured the ergodicity time as a function of  $N$ . Figure 1 shows the respective results for lattices  $12 \times 12$  and  $24 \times 24$ . These results suggest avoiding the steep increase at small  $N$  by choosing  $N$  slightly above the minimum. Thus, we put  $N = 1.25L$  in our simulations. This is in accordance with the remark in Sec. II that one should have  $N \sim L$  and it turns out to be appropriate on all lattices considered.

On smaller lattices, we have used the first method to get the new  $\beta_n$  described in Sec. II. On large lattices, the second one involving reweighting, which performs better for larger  $N$ , has been applied.

For lattices with  $L \geq 24$ , we find effects caused by the occurrence of metastable spin-glass states. Since  $g_n =$

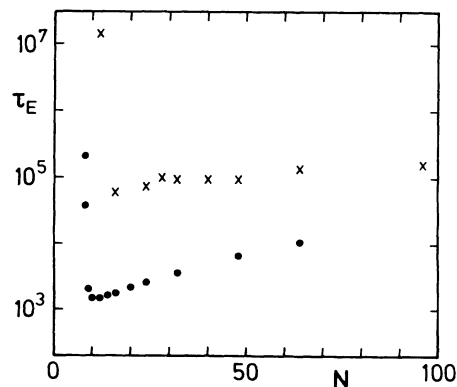


FIG. 1. Ergodicity time  $\tau_E$  as a function of  $N$  for lattices  $12 \times 12$  (dots) and  $24 \times 24$  (crosses).

$\beta_n f_n$ , where  $f_n$  is the free energy, one should have

$$\frac{\Delta g}{\Delta \beta} = H_0 \quad \text{for} \quad \beta \gg 1, \quad (3.1)$$

where  $H_0$  is the ground-state energy. In our calculations  $(g_N - g_{N-1})/(\beta_N - \beta_{N-1})$  turns out to be, in fact, with good accuracy an integer number. However, one actually relies on the lowest energy which has been reached in the Monte Carlo sweeps, which might be larger than  $H_0$  and thus lead to a wrong determination of the parameters.

To see the serious trouble this can cause, suppose that

$$\frac{g_N - g_{N-1}}{\beta_N - \beta_{N-1}} = H_0 + \Delta H, \quad (3.2)$$

with  $\Delta H > 0$  (where  $\Delta H$  can take the values 4, 8, ...). The probability to get from state  $N$  (related to the largest  $\beta$ ) to state  $N - 1$  is  $\min(p_A, 1)$  with  $p_A = \exp[-(\beta_{N-1} - \beta_N)H + (g_{N-1} - g_N)]$ , which after inserting (3.2) becomes

$$p_A = \exp[(\beta_N - \beta_{N-1})(H - H_0 - \Delta H)]. \quad (3.3)$$

From (3.3) it is seen that if in the course of the simulations a true ground state with  $H = H_0$  is reached, the probability for the transition from  $N$  to  $N - 1$  becomes extremely small, i.e., the system gets trapped at low temperature.

Therefore, special care is needed to avoid a wrong determination of type (3.2) of the parameters. For this reason, we have done a large number of iterations in each of which we have determined the set of parameters and an estimate of the ergodicity time  $\tau_E$ . Out of these sets, we have selected the set of parameters associated to the smallest  $\tau_E$ , which in addition has satisfied the requirement

$$\left| \frac{g_N - g_{N-1}}{\beta_N - \beta_{N-1}} - H_0 \right| < \epsilon. \quad (3.4)$$

In (3.4) for  $H_0$ , the lowest energy reached in all previous iterations has been inserted, which has turned out to be a workable concept. Because, as already pointed out, for  $\Delta g/\Delta \beta$ , we find integers with good accuracy,  $\epsilon = 0.1$  is a reasonable bound. The iterations have been terminated

if after an appropriate time no set of parameters with still lower  $\tau_E$  and respecting (3.4) has occurred.

On the largest lattices which we have considered, to reach sufficient accuracy of the parameters in the iterations has turned out to be cumbersome. If the parameters used in a simulation are not accurate enough, the sweeps happen to get restricted to a subinterval of the  $n$  interval, which spoils the calculation.

#### IV. NUMERICAL RESULTS

Our simulations have been performed on 2D lattices with periodic boundary conditions of sizes  $L = 4, 12, 24, 32, 48$  for ten samples of  $J_{ij}$  configurations in each case. This has been done for  $0.3 \leq \beta \leq 3.5$ , setting  $N = 1.25L$ . The ground-state energy density

$$E_0 = \frac{1}{L^2} \min_s \left( - \sum_{\langle ij \rangle} J_{ij} s_i s_j \right), \quad (4.1)$$

the distribution  $P(q)$  of the order parameter (1.2), and the ergodicity time  $\tau_E$  have been determined. From the obtained data, the moments  $\langle q^2 \rangle$  and  $\langle q^4 \rangle$  of  $P(q)$  and the Binder parameter

$$B_q = \frac{1}{2} \left( 3 - \frac{\langle q^4 \rangle}{\langle q^2 \rangle^2} \right), \quad (4.2)$$

have been calculated. The results of this for  $\beta = 3.5$  are presented in Tables I–V. For the samples the errors of the listed quantities are statistical ones including the effect of autocorrelations (the  $E_0$  are exact). The errors of the mean values are the ones derived from the fluctuations of the sample values.

Our results for the mean value of the ground-state energy within errors agree with the numbers of other authors [1,10,12]. However, due to the heating and cooling of the system involved, we expect that our method pro-

TABLE I. Numerical results for  $4 \times 4$  lattice.

Sample no.	$\tau_E$	$E_0$	$\langle q^2 \rangle$	$\langle q^4 \rangle$	$B_q$
1	70.53(8)	-1.125	0.2419(6)	0.1247(5)	0.435(9)
2	92.00(11)	-1.500	0.88256(29)	0.7927(5)	0.9912(7)
3	99.84(13)	-1.375	0.7986(4)	0.6642(7)	0.9793(10)
4	78.39(9)	-1.250	0.4477(6)	0.2767(6)	0.8099(35)
5	64.05(7)	-1.000	0.1746(4)	0.07206(30)	0.318(11)
6	86.01(10)	-1.750	1.00000(1)	1.00000(1)	1.0000(1)
7	85.88(10)	-1.375	0.6620(6)	0.4923(7)	0.9383(18)
8	212.2(4)	-1.250	0.99983(4)	0.99979(5)	1.0000(1)
9	89.02(11)	-1.375	0.6956(4)	0.5174(6)	0.9653(13)
10	100.28(13)	-1.250	0.5237(10)	0.4372(10)	0.703(5)
Mean	97(13)	-1.33(7)	0.64(9)	0.54(10)	0.81(8)

TABLE II. Numerical results for  $12 \times 12$  lattice.

Sample no.	$\tau_E$	$E_0$	$\langle q^2 \rangle$	$\langle q^4 \rangle$	$B_q$
1	1689(14)	-1.3611	0.351(4)	0.1660(28)	0.826(15)
2	4576(61)	-1.3611	0.458(5)	0.248(5)	0.911(25)
3	2818(30)	-1.4444	0.778(2)	0.610(2)	0.996(4)
4	3509(42)	-1.3611	0.481(7)	0.311(7)	0.83(4)
5	8421(153)	-1.3333	0.592(4)	0.360(4)	0.986(12)
6	1219(8)	-1.3750	0.2250(27)	0.0872(17)	0.64(4)
7	3944(49)	-1.3472	0.5097(32)	0.2793(33)	0.962(13)
8	1271(9)	-1.3472	0.2732(29)	0.1210(19)	0.690(30)
9	2722(29)	-1.4861	0.7842(31)	0.640(4)	0.980(8)
10	1360(10)	-1.4444	0.302(4)	0.1656(31)	0.59(4)
Mean	3153(695)	-1.386(17)	0.48(6)	0.30(6)	0.84(5)

TABLE III. Numerical results for  $24 \times 24$  lattice.

Sample no.	$\tau_E$	$E_0$	$\langle q^2 \rangle$	$\langle q^4 \rangle$	$B_q$
1	31963(516)	-1.3958	0.472(5)	0.255(5)	0.929(24)
2	55208(1175)	-1.4271	0.430(9)	0.225(7)	0.89(5)
3	184218(7176)	-1.3993	0.532(38)	0.314(33)	0.94(14)
4	76188(1905)	-1.4028	0.576(3)	0.342(4)	0.985(11)
5	108775(3289)	-1.4167	0.619(2)	0.393(2)	0.986(7)
6	43150(826)	-1.3958	0.329(5)	0.130(3)	0.898(30)
7	97243(2810)	-1.4271	0.524(5)	0.304(5)	0.946(18)
8	192333(7852)	-1.3958	0.401(31)	0.250(21)	0.72(17)
9	109485(3291)	-1.4063	0.599(6)	0.382(7)	0.968(20)
10	40648(751)	-1.3889	0.328(8)	0.167(6)	0.72(7)
Mean	93921(18067)	-1.406(4)	0.481(34)	0.276(28)	0.900(31)

TABLE IV. Numerical results for  $32 \times 32$  lattice.

Sample no.	$10^{-5} \tau_E$	$E_0$	$\langle q^2 \rangle$	$\langle q^4 \rangle$	$B_q$
1	3.73(10)	-1.4082	0.500(15)	0.271(14)	0.96(6)
2	15.0(6)	-1.3906	0.43(4)	0.208(33)	0.93(20)
3	11.0(5)	-1.3867	0.348(13)	0.177(7)	0.77(8)
4	1.147(16)	-1.4277	0.229(5)	0.099(3)	0.55(7)
5	2.73(5)	-1.4121	0.443(6)	0.217(5)	0.949(29)
6	8.74(34)	-1.4082	0.447(20)	0.250(14)	0.88(9)
7	5.79(17)	-1.3945	0.658(6)	0.438(8)	0.994(10)
8	3.45(8)	-1.4063	0.162(14)	0.049(7)	0.57(29)
9	5.83(16)	-1.3965	0.576(11)	0.343(10)	0.983(34)
10	2.60(5)	-1.4121	0.490(6)	0.268(5)	0.941(23)
Mean	6.0(14)	-1.404(4)	0.43(5)	0.232(35)	0.85(5)

TABLE V. Numerical results for  $48 \times 48$  lattice.

Sample no.	$10^{-6} \tau_E$	$E_0$	$\langle q^2 \rangle$	$\langle q^4 \rangle$	$B_q$
1	4.83(27)	-1.3967	0.304(8)	0.117(5)	0.87(6)
2	12.0(10)	-1.3967	0.054(10)	0.004(3)	0.74(79)
3	5.5(3)	-1.4115	0.35(1)	0.131(7)	0.98(6)
4	2.81(15)	-1.4054	0.143(12)	0.021(6)	0.99(24)
5	2.06(11)	-1.3906	0.23(5)	0.086(26)	0.71(57)
6	6.3(4)	-1.4063	0.48(22)	0.26(19)	0.93(92)
7	6.02(34)	-1.4019	0.549(23)	0.316(20)	0.98(8)
8	1.00(4)	-1.3845	0.370(7)	0.146(5)	0.97(4)
9	9.2(7)	-1.4115	0.42(4)	0.18(4)	0.97(20)
10	5.1(3)	-1.3976	0.28(4)	0.085(27)	0.94(35)
Mean	5.5(10)	-1.4003(28)	0.32(4)	0.135(31)	0.91(3)

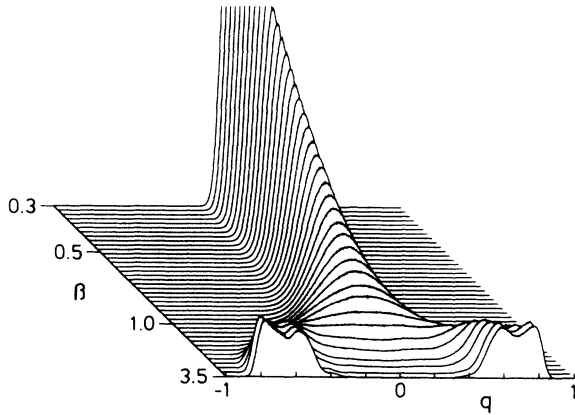


FIG. 2. Order-parameter distribution  $P(q, \beta)$  for sample 5 on the  $32 \times 32$  lattice.

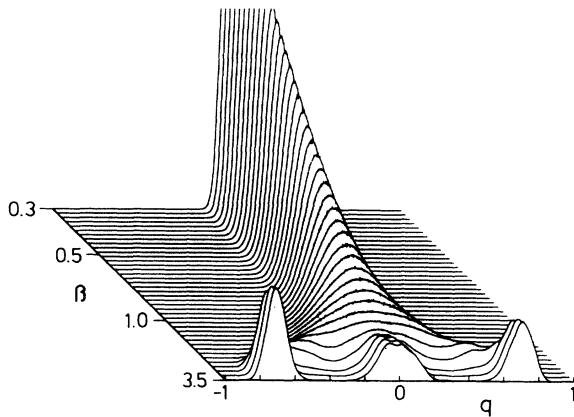


FIG. 3. Order-parameter distribution  $P(q, \beta)$  for sample 3 on the  $32 \times 32$  lattice.

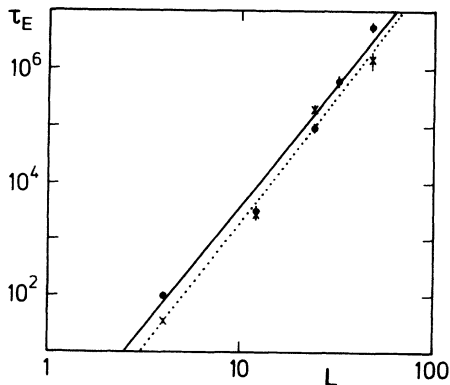


FIG. 4. Dependence of  $\tau_E$  on the lattice size  $L$  for simulated tempering (dots, fit solid line) and the multicanonical method (crosses, fit dashed line).

vides more reliable results than other methods. In this context, we also find that simulated tempering, in addition, is an advantageous tool for the exploration of the ground-state structure.

Our results for  $\langle q^2 \rangle$  and  $B_q$  are compatible with those given by Berg and Celik [1], though they are generally slightly larger. A possible reason for this is that we have measured at a lower temperature than they did. From our tables it is seen that there are strong dependences on the particular sample as is expected because of the lack of self-averaging [4-6].

The invariance of the Hamiltonian under the transformation  $s_i \rightarrow s_i, t_i \rightarrow -t_i$  requires  $P(q) = P(-q)$ . This provides a test of ergodicity. Failure to pass this test signals ergodicity breaking in conventional approaches. Further details of  $P(q)$  at low temperatures cannot be predicted since the value of  $q$  is sensitive to the particular ground state and the ground states are not related by a global symmetry of the Hamiltonian.

Figures 2 and 3 show typical results for the distribution  $P(q)$ . The relation  $P(q) = P(-q)$  is respected by these distributions, which confirms the ergodicity of our algorithm. It can also be seen that the form of the distribution depends on the configuration of couplings even for rather large lattices. The scaling law [13]  $P(q) = L^{0.1} \bar{P}(qL^{0.1})$  with an universal function  $\bar{P}$  was verified (due to the low number of samples with relatively large errors).

The dependence of the ergodicity time on the lattice size  $L$  is depicted in Fig. 4 and compared to the multicanonical data given by Berg and Celik [1]. We get the dependence

$$\tau_E \sim L^{4.27(8)}. \quad (4.3)$$

A fit of the form  $\tau_E \sim \exp(kL)$  is not possible. Our ergodicity times are comparable with those of Ref. [1] [where the dynamical critical exponent 4.4(3) is obtained]. However, because our computer programs can be fully vectorized in terms of CPU times, we gain a large factor.

We compare our results with those of Berg and Celik [1] because this is straightforward and because these most recent results are considered to constitute major progress. As Berg and Celik point out, the comparison to some standard simulations is not entirely straightforward. We refer to their work for details of this.

The scaling law (4.3) with respect to the scaling law  $\tau \sim L^6$  reported [4] for the Metropolis algorithm constitutes a considerable improvement. However, most importantly one has to realize that by Metropolis one does not get ergodicity and thus cannot reach equilibrium.

## ACKNOWLEDGMENTS

This work has been supported in part by the Deutsche Forschungsgemeinschaft through Grant Nos. Ke 250/7-1 and Ke 250/7-2. The computations have been done on the SNI 400/40 of the Universities of Hessen at Darmstadt and on the Convex C230 of Marburg University.

- [1] B.A. Berg and T. Celik, *Phys. Rev. Lett.* **69**, 2292 (1992); *Int. J. Mod. Phys. C* **3**, 1251 (1992).
- [2] B.A. Berg and T. Neuhaus, *Phys. Lett. B* **67**, 249 (1991); *Phys. Rev. Lett.* **68**, 9 (1992).
- [3] E. Marinari and G. Parisi, *Europhys. Lett.* **19**, 451 (1992).
- [4] K.H. Fischer and J.A. Hertz, *Spin Glasses* (Cambridge University Press, Cambridge, 1991).
- [5] K. Binder and A.P. Young, *Rev. Mod. Phys.* **58**, 801 (1986).
- [6] M. Mezard, G. Parisi, and M.A. Virasoro, *Spin Glass Theory and Beyond* (World Scientific, Singapore, 1987).
- [7] N. Metropolis, A.W. Rosenbluth, M.N. Rosenbluth, A.H. Teller, and E. Teller, *J. Chem. Phys.* **21**, 1087 (1953).
- [8] W. Kerler and A. Weber, *Phys. Rev. B* **47**, R11563 (1993).
- [9] A.M. Ferrenberg and R.H. Swendsen, *Phys. Rev. Lett.* **61**, 635 (1988); E. Marinari, *Nucl. Phys. B* **235** [FS 11], 123 (1984).
- [10] J.S. Wang and R.H. Swendsen, *Phys. Rev. B* **38**, 4840 (1988).
- [11] W.H. Press, B.P. Flannery, S.A. Teukolsky, and W.T. Vetterling, *Numerical Recipes* (Cambridge University Press, Cambridge, 1986).
- [12] H.F. Cheng and W.L. McMillan, *J. Phys. C* **16**, 7027 (1983).
- [13] R.N. Bhatt and A.P. Young, *Phys. Rev. B* **37**, 5606 (1988).